Modeling Multifractality of the Solar Wind

Wiesław M. Macek

Space Research Centre
Polish Academy of Sciences
Bartycka 18 A, 00-716 Warsaw, Poland
e-mail: macek@cbk.waw.pl
http://www.cbk.waw.pl/∼macek

Abstract

The question of multifractality is of great importance because it allows to investigate interplanetary hydromagnetic turbulence. Starting from Richardson's version of turbulence, many authors try to recover the observed scaling exponents, using various models of the turbulence cascade for the dissipation rate. The multifractal spectrum has been investigated with Voyager (magnetic field) data in the outer heliosphere and with Helios (plasma) data in the inner heliosphere. A direct determination of the multifractal spectrum from the data is known to be a difficult problem. Following other applications, we use the Grassberger and Procaccia method that allows calculation of the generalized dimensions of the solar wind attractor in the phase space directly from the cleaned experimental signal. We analyse time series of plasma parameters of the low-speed streams of the solar wind measured in situ by Helios 2 in the inner heliosphere. We demonstrate that the influence of noise in the data can be efficiently reduced by a singular-value decomposition filter.

The resulting spectrum of dimensions shows multifractal structure of the solar wind attractor. In order to quantify that multifractality, we use a simple analytical model of the dynamical system. Namely, we consider the generalized self-similar baker's map with two parameters describing uniform compression and natural invariant measure on the attractor of the system. The action of this map exhibits stretching and folding properties leading to sensitive dependence on initial conditions. The obtained solar wind singularity spectrum is consistent with that for the multifractal measure on the weighted baker's map. The values of the parameters fitted demonstrates small dissipation of our dynamical system and shows that some cubes that cover the attractor in phase space are visited at least one order of magnitudes more frequently than other cubes.

This work has been supported by the
State Scientific Research Committee through Grant No. 2 P03B 126 24

Fractals

A **FRACTAL** is a rough or fragmented geometrical shape that can be subdivided in parts, each of which is (at least approximately) a reduced-size copy of the whole.

Fractals are generally *self-similar* and independent of scale.

Chaos and attractors

CHAOS ($\chi\alpha o\varsigma$) is

- APERIODIC long-term behavior
- in a DETERMINISTIC system
- that exhibits SENSITIVITY TO INITIAL CONDITIONS.

A positive finite Lyapunov exponent (metric entropy) implies chaos.

An **ATTRACTOR** is a *closed* set A with the properties:

1. A is an INVARIANT SET:
   any trajectory $\mathbf{x}(t)$ that start in A stays in A for ALL time t.
2. A ATTRACTS AN OPEN SET OF INITIAL CONDITIONS:
   there is an open set U containing A ($\subset U$) such that if $\mathbf{x}(0) \in U$, then the distance from $\mathbf{x}(t)$ to A tends to zero as $t \to \infty$.
3. A is MINIMAL:
   there is NO proper subset of A that satisfies conditions 1 and 2.

Introduction

The generalized dimensions of attractors are important characteristics of *complex* dynamical systems. Since these dimensions are related to frequencies with which typical orbits in phase space visit different regions of the attractors, they can provide information about dynamics of the systems. More precisely, one may distinguish a probability measure from its geometrical support, which may or may not have fractal geometry. Then, if the measure has different fractal dimensions on different parts of the support, the measure is multifractal. The modern technique of nonlinear time series analysis allows to estimate the multifractal measure directly from a single time series.

The question of multifractality is of great importance also for the solar wind community, because it allows to investigate the nature of interplanetary hydromagnetic turbulence (e.g., Burlaga, 1991; Marsch et al., 1996). The solar wind plasma flowing supersonically away from the Sun is well modeled within the framework of the hydromagnetic theory. This continuous flow has two forms: slow (≈ 400 km s^{-1}) and fast (≈ 700 km s^{-1}). The fast wind is associated with coronal holes and is relatively uniform and stable, while the slow wind is quite variable. We limit our study to the low-speed stream.

Indication for a chaotic attractor in the slow solar wind has been given: Macek (1998) has calculated the correlation dimension of the reconstructed attractor and has provided tests for *nonlinearity* in the solar wind data, including a powerful method of singular-value decomposition, and statistical surrogate data tests. Macek and Redaelli (2000) have shown that the Kolmogorov entropy of the attractor is *positive* and finite, as it holds for a *chaotic* system. The entropy is constrained by a *positive* Lyapunov exponent that exhibits sensitive to initial conditions of the system (Redaelli and Macek, 2001).

- W. M. Macek, Physica D 122, 254–264 (1998).
- W. M. Macek and S. Redaelli, Phys. Rev. E 62, 6496–6504 (2000).
- W. M. Macek (ed.), Nonlinear dynamics and fractals in space, special issue, Planet. Space Sci. 49, 1175–1247 (2001).
- S. Redaelli and W. M. Macek, Planet. Space Sci. 49, 1211–1218 (2001).
- W. M. Macek, Multifractality and chaos in the solar wind, in *Experimental Chaos*, edited by S. Boccaletti, B. J. Gluckman, J. Kurths, L. M. Pecora, and M. L. Spano, American Institute of Physics, New York, 2002, Vol. 622, pp. 74–79.
- W. M. Macek, The multifractal spectrum for the solar wind flow, in *Solar Wind 10*, edited by M. Velli, R. Bruno, F. Malara, American Institute of Physics, New York, 2003, vol. 679, pp. 530-533.
- W. M. Macek, R. Bruno, G. Consolini, The generalized dimensions for fluctuations in the solar wind, Physical Review E, in press (2005).

In this paper we have extended our previous results on the dimensional time series analysis (Macek, 1998). Namely, we apply the technique that allows a realistic calculation of the generalized dimensions of the solar wind flow, directly from the cleaned experimental signal by using the Grassberger and Procaccia method. The resulting spectrum of dimensions shows multifractal structure of the solar wind in the inner heliosphere. The obtained multifractal spectrum is consistent with that for the multifractal measure on the self-similar weighted baker's map.

These results provide direct supporting evidence that the *complex* solar wind is likely to have multifractal structure. In this way, we have further supported our previous conjecture that trajectories describing the system in the inertial manifold of phase space asymptotically approach the attractor of low-dimension. One can expect that the attractor in the low-speed solar wind plasma should contain information about the dynamic variations of the coronal streamers. It is also possible that it represents a structure of the time sequence of near-Sun coronal fine-stream tubes (see, Macek, 1998), and references therein.

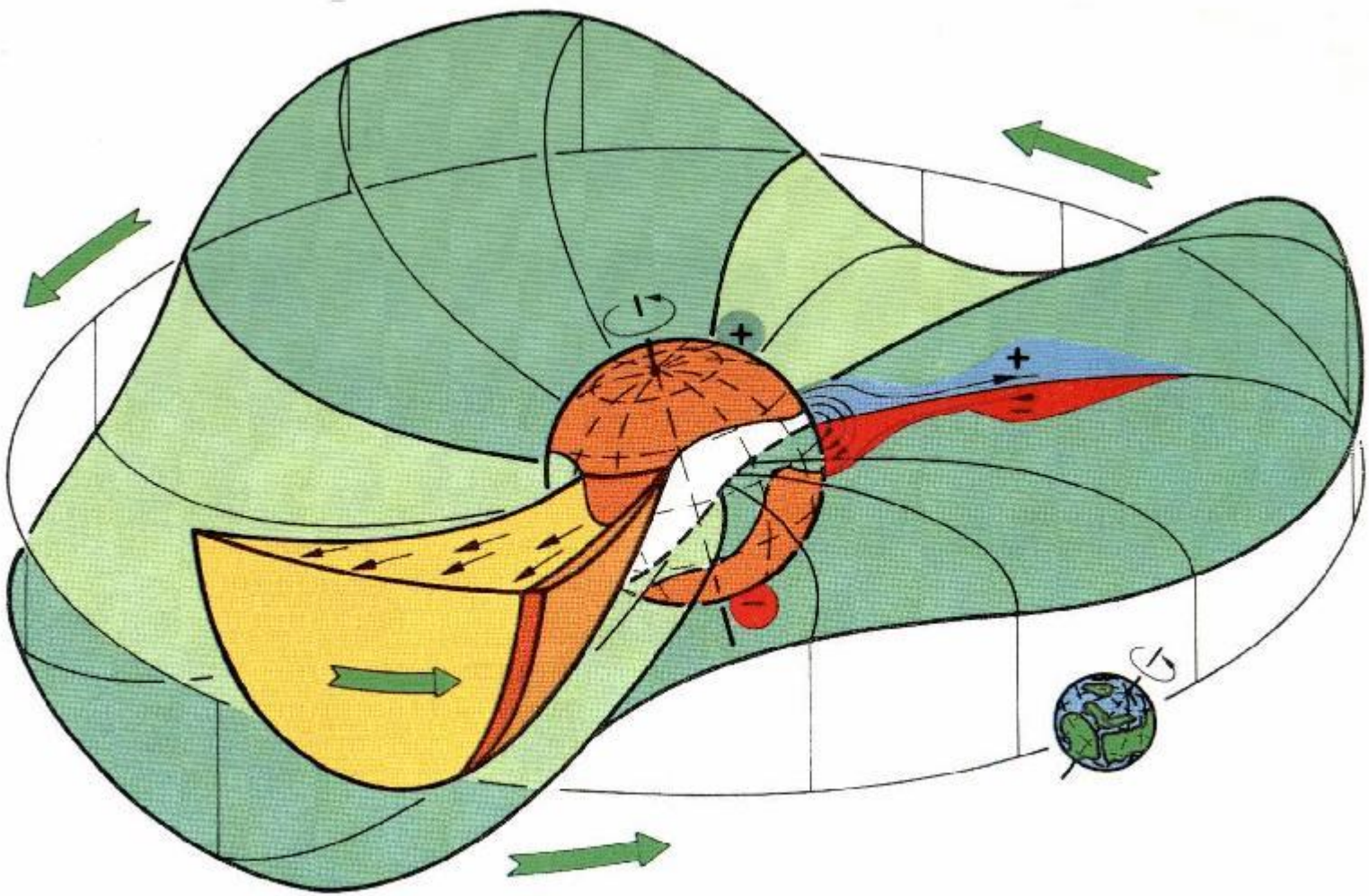

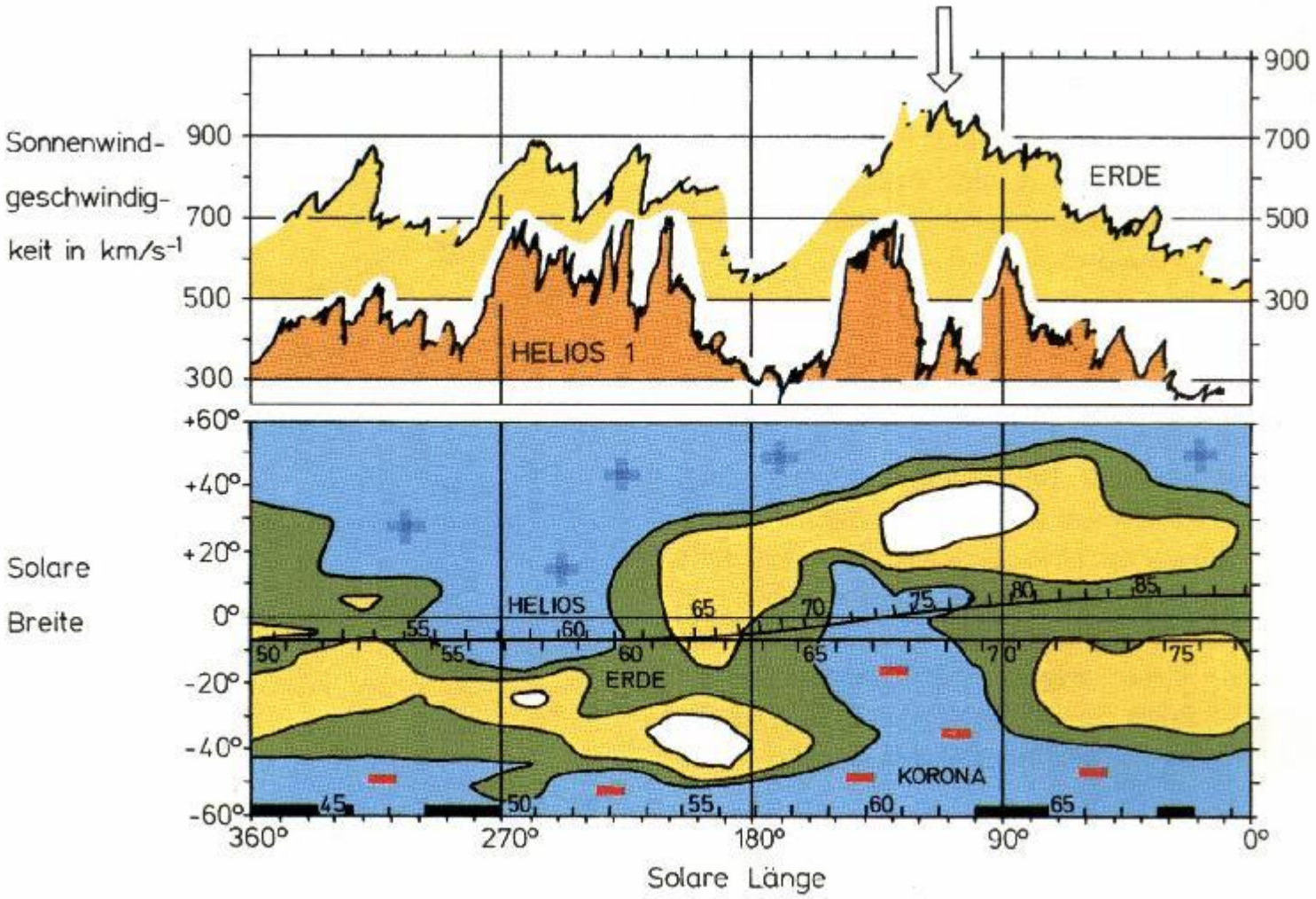
Sonnenwind-
geschwindig-
keit in km/s⁻¹
900
700
500
300
ERDE
HELIOS 1
Solare
Breite
+60°
+40°
+20°
0°
-20°
-40°
-60°
HELIOS
ERDE
KORONA
360°
270°
180°
90°
0°
Solare Länge

Helios 1 and 2

Orbits

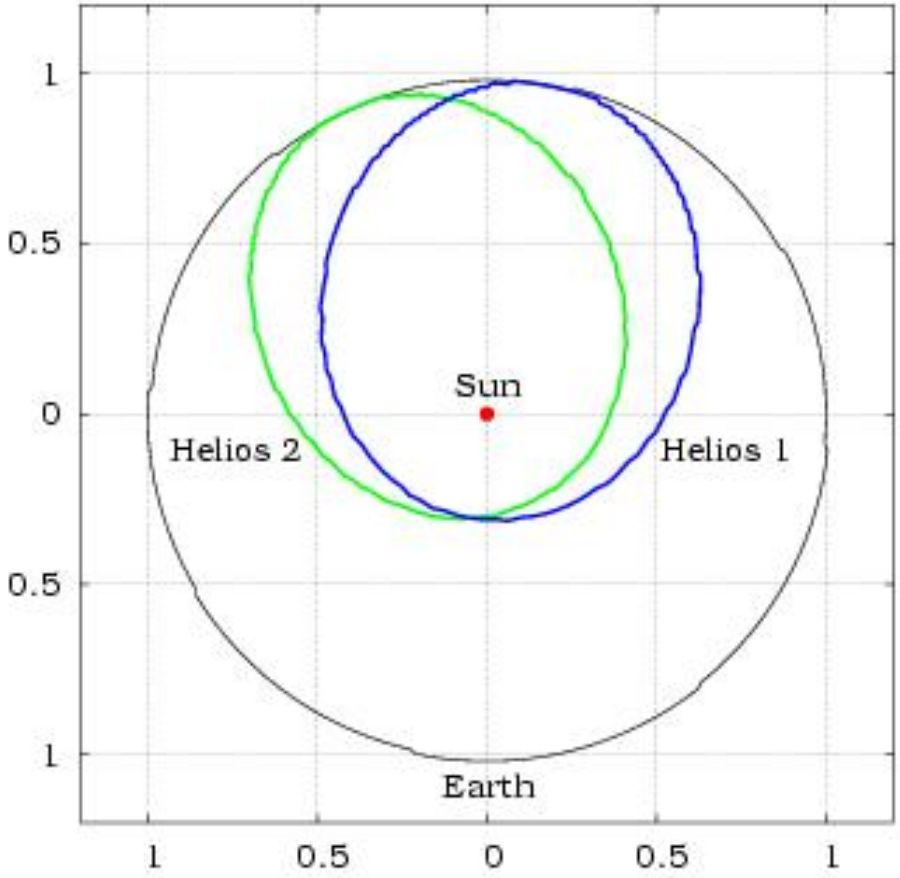

Data

No	Year	From (DOY)	To (DOY)	Distance from the Sun (AU)
I	1977	116	121	0.32
II	1977	348	357	0.84

Sampling time: 40.5 s

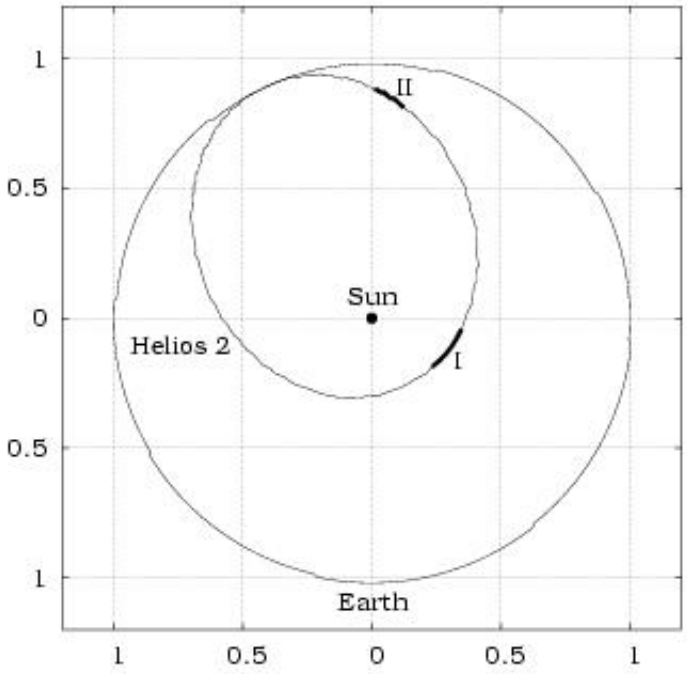

Alfvénic Velocity

Sound velocity: $c_s^2 = \gamma \frac{p}{\rho}$

Magnetic field pressure: $p = \frac{B^2}{8\pi}$

Adiabatic exponent: $\gamma = \frac{f+2}{f} = 2 \quad f = 2$

Alfvénic velocity: $v_A = \frac{B}{\sqrt{4\pi\rho}}$

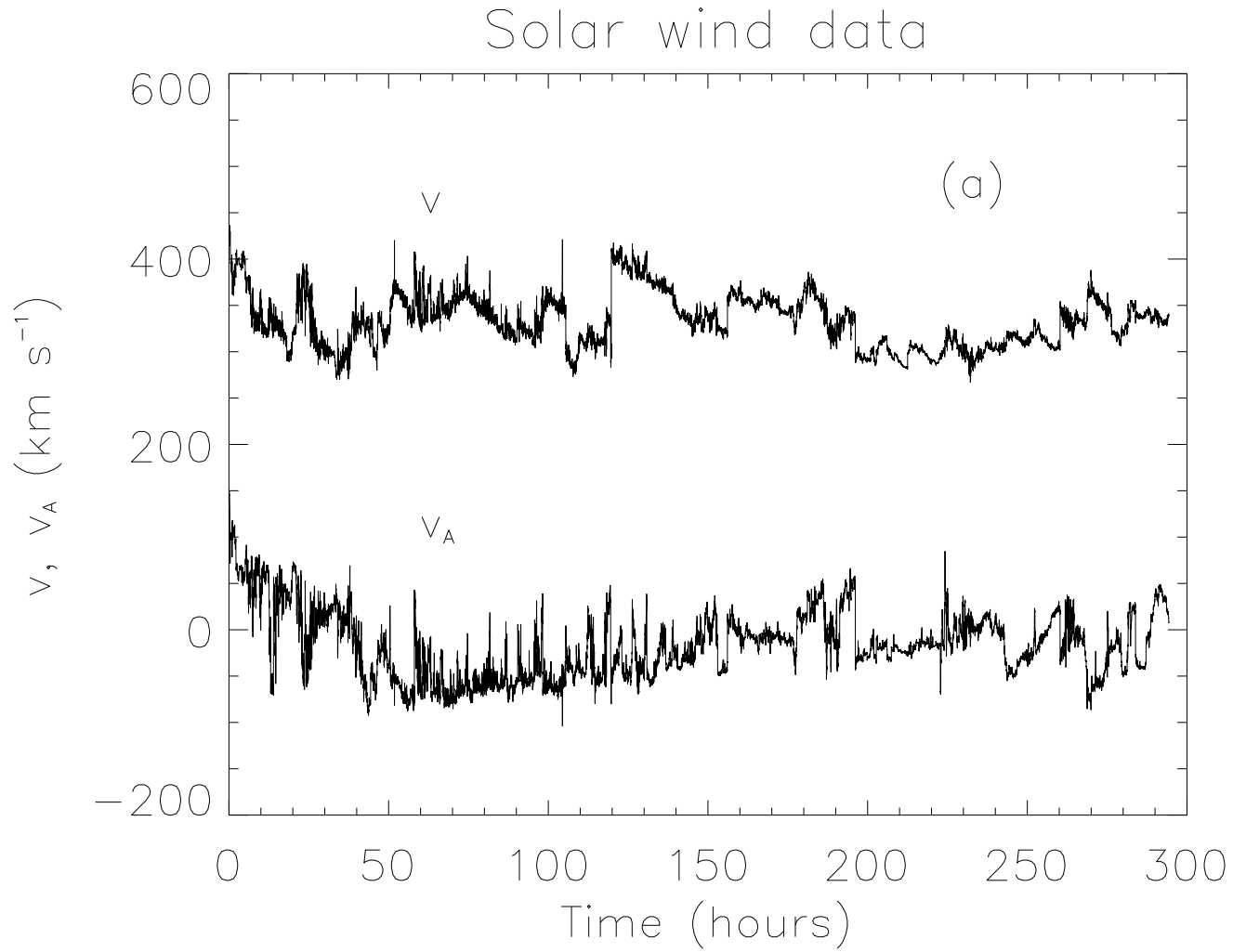

Fig. 1. (a) The raw data of the radial flow velocity with Alfvénic velocity, v and v_A, observed by the Helios 2 spacecraft in 1977 from 116:00 to 121:21 (day:hour) at distances 0.3 AU, and from 348:00 to 357:00 at 0.9 AU from the Sun.

Singular-value decomposition

The normalized vectors $\mathbf{X}(t_i) = [v(t_i), v(t_i+\tau), \ldots, v(t_i+(m-1)\tau)]$ in the embedding phase space of dimension m, where $i = 1, \ldots, n$, $n = N-(m-1)\tau$, number of vectors.

A is the $n \times m$ trajectory matrix $(n \geq m)$

$$A = \frac{1}{\sqrt{n}} \begin{pmatrix} \mathbf{X}(t_1) \\ \mathbf{X}(t_2) \\ \vdots \\ \mathbf{X}(t_n) \end{pmatrix}$$

Decomposition

The matrix $A_{ij} = v(t_i + (j-1)\tau) = UWV^T$, $j = 1, \ldots, m$,
U – $n \times m$ matrix with orthonormal columns, $(U^T U)_{ij} = \delta_{ij}$,
V – $m \times m$ orthonormal matrix, $(V^T V)_{ij} = (VV^T)_{ij} = \delta_{ij}$,
W – $m \times m$ diagonal matrix, $W_{ij} = \delta_{ij}\, w(j)$.

The projection of the original vectors onto the new orthogonal space: $A \rightarrow A^{'} = AV = UW$
the matrix of eigenfunctions $\Psi^{'} = A^{'}W$ and $\Psi = U$.

Normalization, for a given m,

$$\xi_j = w^2(j)/(\sum_{k=1}^{m} w^2(k)) \tag{1}$$

is the variance of the j-th principal component;

Normalization of the eigenfunctions, $j = 1, \ldots, m$,

$$\frac{1}{n} \sum_{i=1}^{n} |\Psi^{'}_{ij}|^2 = {\xi_j}^2 \tag{2}$$

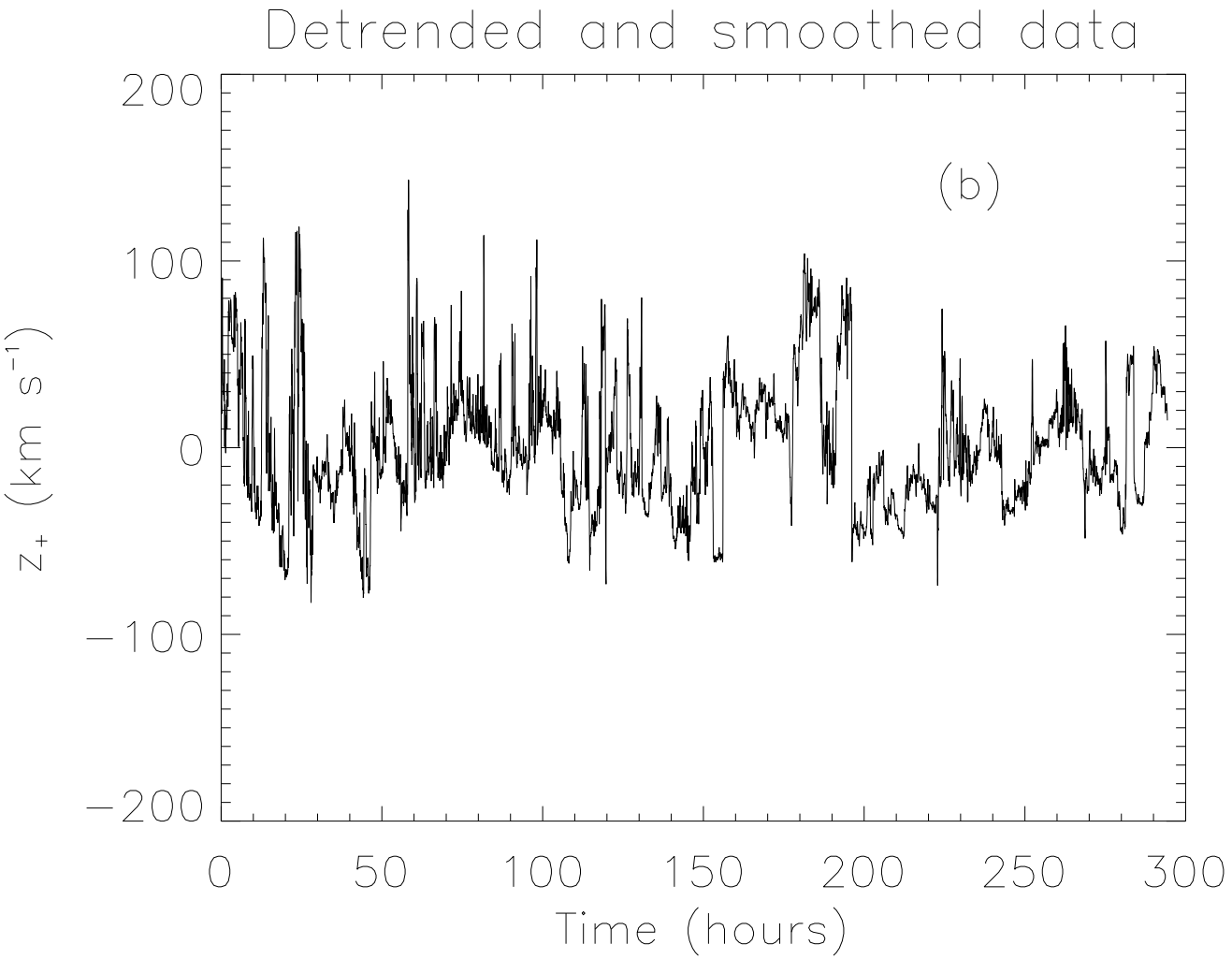

Fig. 1. (b) the Elsässer variable $z_+ = v \pm v_A$ for B_o pointing to/away from the Sun for the detrended and filtered data using singular-value decomposition with five largest eigenvalues.

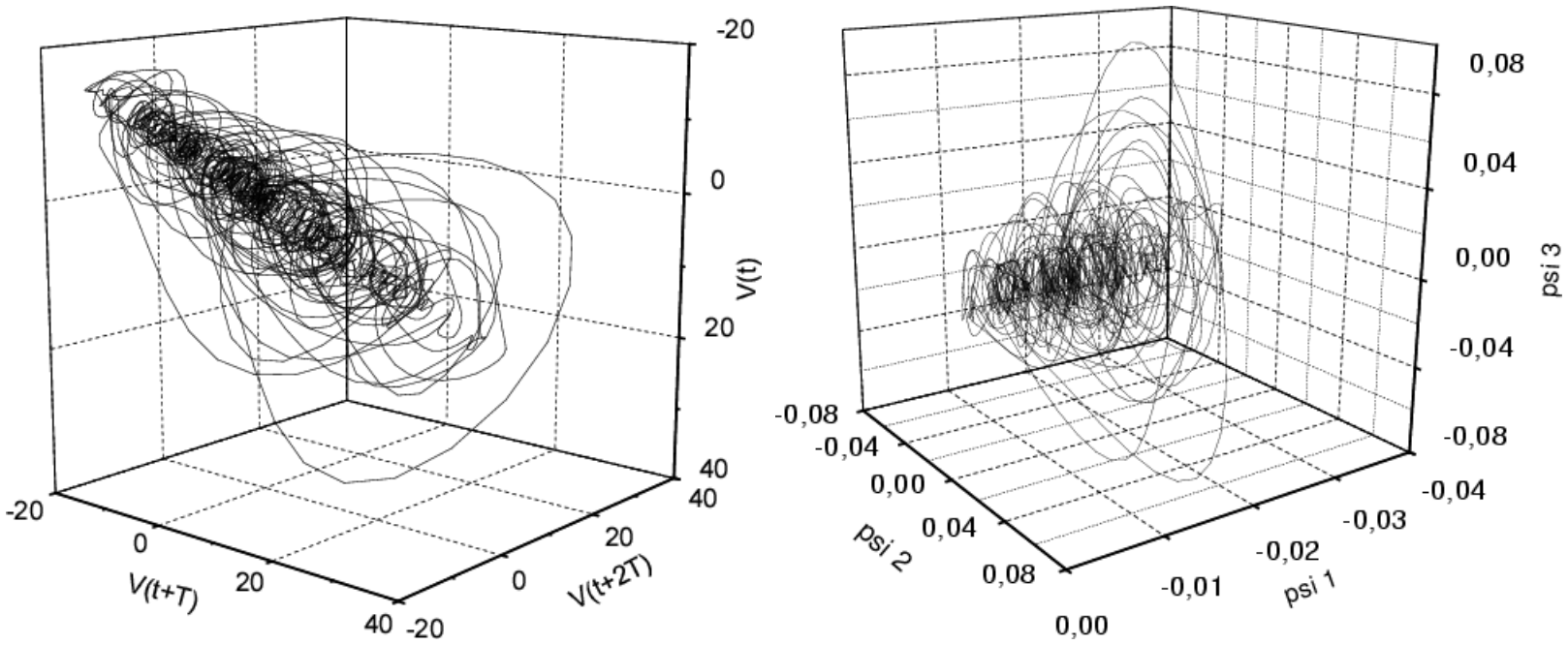

Fig. 2. The projection of the attractor onto the three-dimensional space, reconstructed from the detrended data, $T = 4\ \Delta t$, using (a) the moving average and also (b) the singular-value decomposition filters ($\Psi = U$).

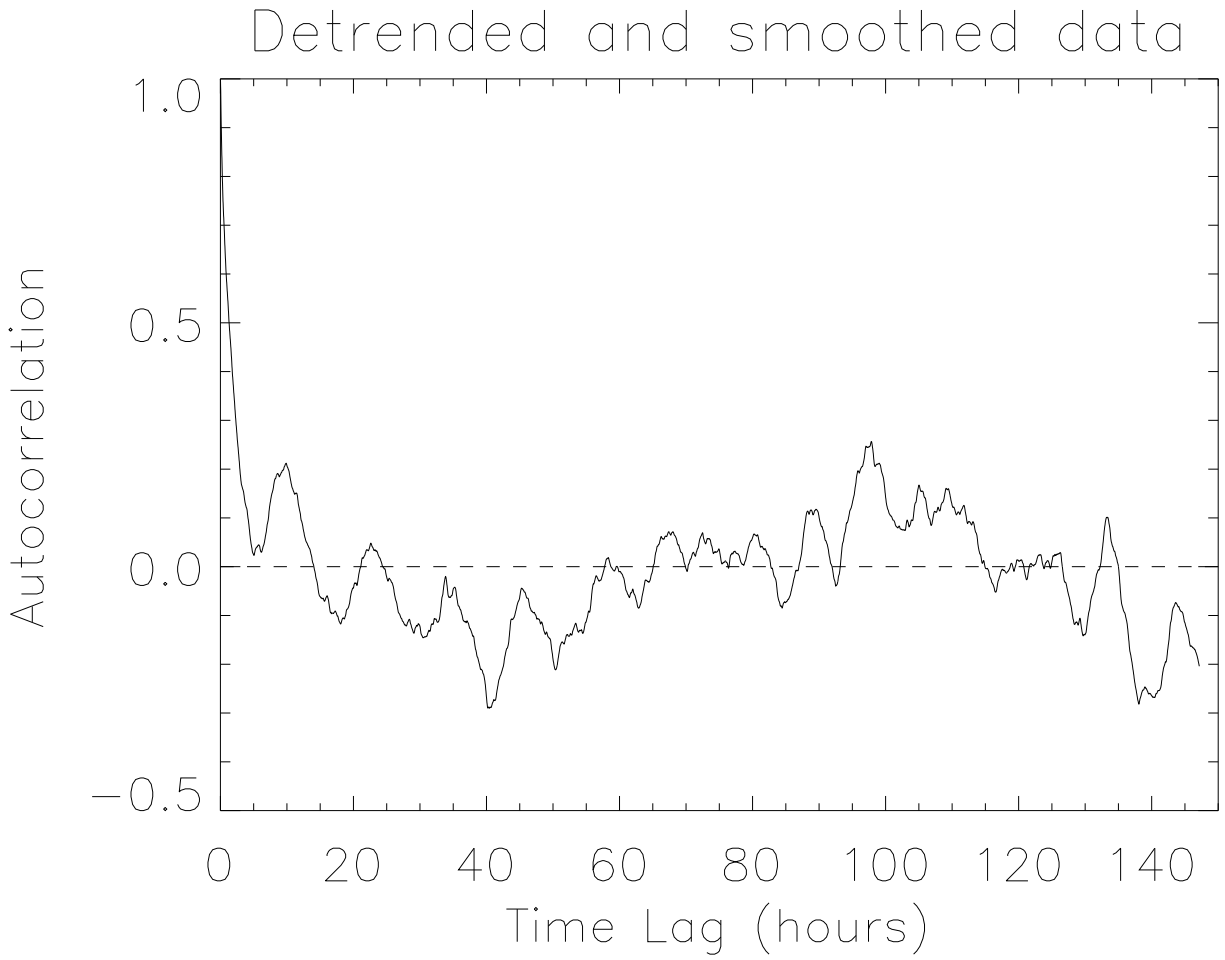

Fig. 3. The normalized autocorrelation function as a function of the time lag for the detrended and filtered data.

Method

Dimensions

$M(r)$, number of hypercubes of size r in the phase space, needed to cover the attractor;
p_k, probability that a point from a time series falls in k-th hypercube;
the q-order function, $k = 1, ..., M$,

$$I_q(r) = \sum_{k=1}^{M} (p_k)^q, \tag{3}$$

the generalized *dimension*

$$D_q = \frac{1}{q-1} \lim_{r \to 0} \frac{\ln I_q(r)}{\ln r} \tag{4}$$

For large m, we have (plateau) a slope ($q = 2$ in eq. (4))

$$D_2 \approx \frac{\ln C_m(r)}{\ln (r)} \tag{5}$$

where the correlation sum is

$$C_m(r) = \frac{1}{n_{\rm ref}} \sum_{i=1}^{n_{\rm ref}} \frac{1}{n-2n_{\rm c}} \sum_{j=n_c+1}^{n} \theta(r - |\mathbf{X}(t_i) - \mathbf{X}(t_j)|) \tag{6}$$

with $\theta(x)$ being the unit step function
$n = N - (m-1)\tau$, for N data points number of vectors
in the m-dimensional embedding space,
$\mathbf{X}(t_i) = [x(t_i), x(t_i + \tau), \ldots, x(t_i + (m-1)\tau)]$, where $x = v \pm v_A$,
with the radial velocity v, the Alfvénic velocity $v_A = B/(\mu_o \rho)^{1/2}$
(radial component of the magnetic field B and mass density ρ)
τ, delay time (characteristic time of autocorrelation function)
$n_{\rm ref} = 5000$ is the number of reference points,
$n_{\rm c} = 4$ is the *Theiler* correction.

The average slope for $6 \leq m \leq 10$ is taken as D_2.

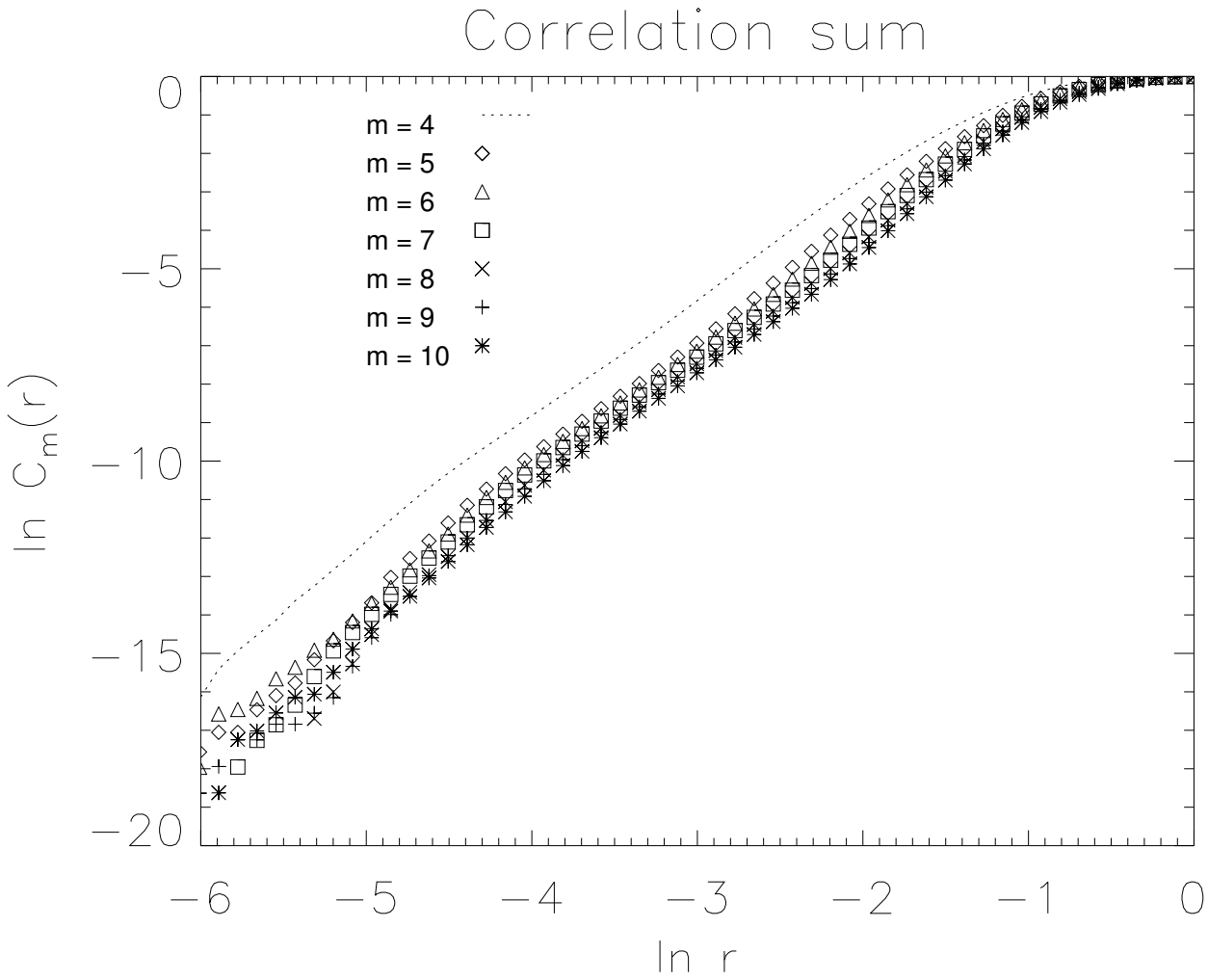

Fig. 4. The natural logarithm of the correlation sum $C_m(r)$ versus $\ln r$ (normalized) obtained for the cleaned experimental signal is shown for various embedding dimensions: $m = 4$ (dotted curve), $m = 5$ (diamonds), 6 (triangles), 7 (squares), 8 (crosses), 9 (plus), and 10 (stars).

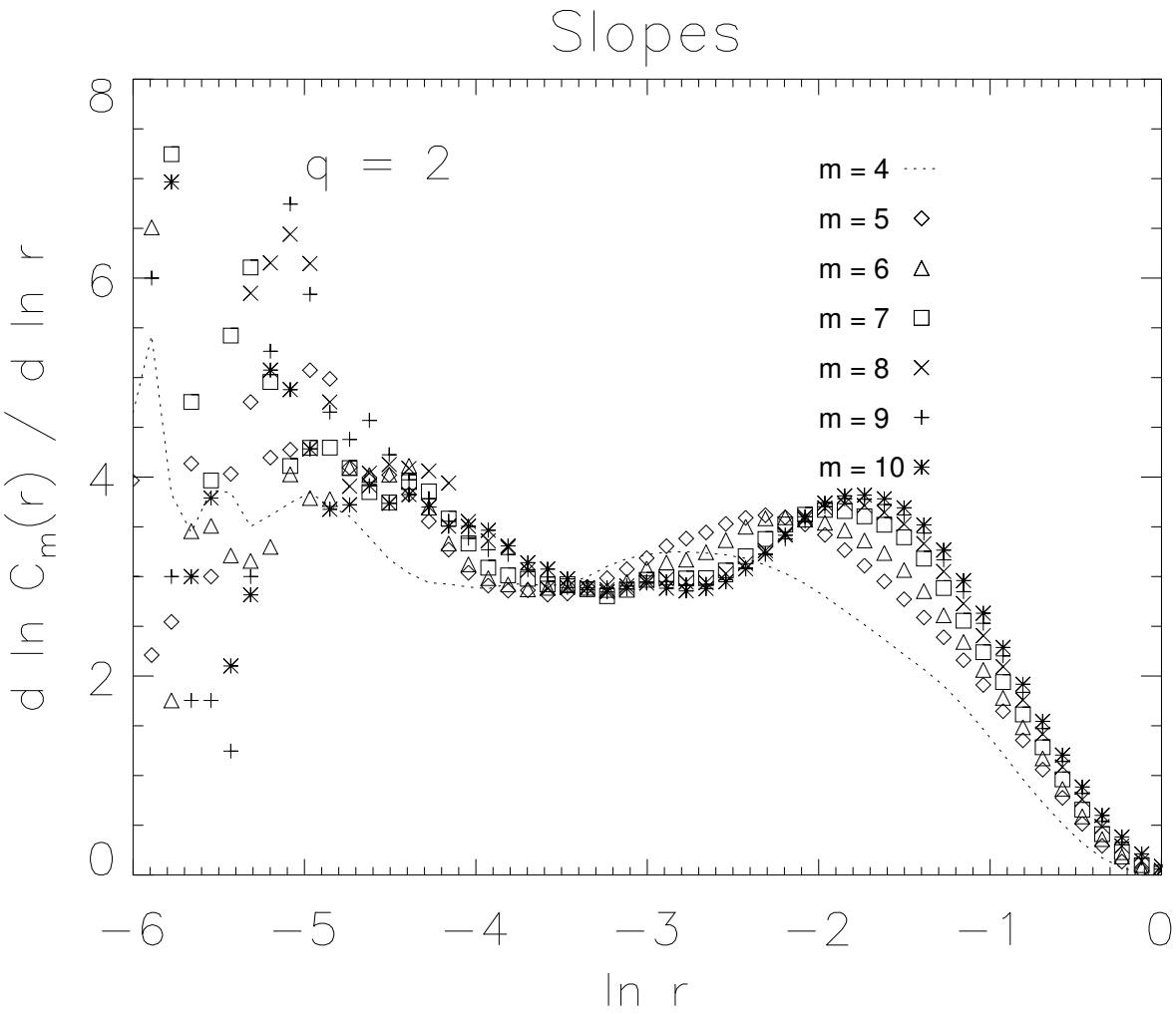

Fig. 5. The slopes $D_{2,m}(r) = \mathrm{d}(\ln C_m(r))/\mathrm{d}(\ln r)$ of the correlation sum $C_m(r)$ versus $\ln r$ (normalized) obtained for detrended and filtered data are shown for various embedding dimensions m.

Weighted average: $I_q(r) = \sum p_j (p_j)^{q-1} = \langle (p_j)^{q-1} \rangle$
the generalized average probability per hypercube: $\sqrt[q-1]{\langle (p_j)^{q-1} \rangle}$.

- $q = 0$, the capacity dimension, D_0
- $q \to 1$, geometrical average, the information dimension
- $q = 2$, arithmetic average, the correlation dimension
- $q = 3$, root-mean-square average

High order dimensions quantify the multifractality
of the probability measure on the attractor.

In practice, for a given m and r,

$$p_j \simeq \frac{1}{n-2n_c-1} \sum_{i=n_c+1}^{n} \theta(r- \mid \mathbf{X}(t_i) - \mathbf{X}(t_j) \mid) \tag{7}$$

with $\theta(x)$ being the unit step function; $\mathbf{X}(t_j)$ denotes one of $n = N-(m-1)\tau$ vectors in the m-dimensional embedding space,
$\mathbf{X}(t_i) = [v(t_i), v(t_i+\tau), \ldots, v(t_i+(m-1)\tau)]$,
τ, delay time, characteristic time of autocorrelation function.
$I_q(r)$ is equal to the generalized q-point correlation sum

$$C_q(m,r) \; = \; \frac{1}{n_{\mathrm{ref}}} \sum_{j=1}^{n_{\mathrm{ref}}} (p_j)^{q-1} \tag{8}$$

where $n_{\mathrm{ref}} = 5000$ is the number of reference vectors.

For large m and small r in the scaling region

$$C_q(m,r) \propto r^{(q-1)D_q} \exp(-m\tau K_q) \tag{9}$$

D_q and K_q are approximations of the limit $r \to 0$ in Eq. (4).
The average slope for $6 \leq m \leq 10$ is taken as $(q-1)D_q$.

TABLE 1. Solar wind velocity fluctuations* data	
Number of data points, N	26163
Sampling time, Δt	40.5 s
Skewness†, κ_3	0.59
Kurtosis†, κ_4	0.37
Minimum frequency	9.4 $\times 10^{-7}$ Hz
Dominant frequency	2.5 $\times 10^{-5}$ Hz
Maximum frequency	1.2 $\times 10^{-2}$ Hz
Relative complexity‡	0.1
Autocorrelation time§, t_{a}	7.1 $\times 10^{3}$ s
Correlation dimension¶, D_2	3.35 ± 0.21
Entropy‡¶, $(q = 2), K_2$	0.1
Largest Lyapunov exponent‡¶, $\lambda_{\max}$	1/4 – 1/3
Predictability horizon time‡	3 $\times 10^{4}$ s

*Slow trends (1) $344.596 - 20.291\,t - 0.358\,t^2$, and $88.608 - 452.349\,t + 343.471\,t^2$ (2) $397.847 - 291.602\,t - 241.999\,t^2$, and $-30.050 + 87.756\,t - 77.773\,t^2$ (with t being a fraction of a given sample) were subtracted from the original data, $v(t_i)$ and $v_A(t_i)$, in km s^{-1}, and the data were (8-fold) smoothed using moving averages and singular-value decomposition with five eigenvalues. The resulting range of data $x_{\max} - x_{\min} = 226.4$ km s^{-1}.

†The third and fourth moments of the distribution function are (with average velocity $\langle x \rangle = 0.622$ km s^{-1} and standard deviation $\sigma = 33.514$ km s^{-1})

$$\kappa_3 = \frac{1}{N}\sum_{i=1}^{N}\left[\frac{x_i - < x >}{\sigma}\right]^3, \quad \kappa_4 = \frac{1}{N}\sum_{i=1}^{N}\left[\frac{x_i - < x >}{\sigma}\right]^4 - 3$$

‡Approximately.

§The autocorrelation time t_a is given by $(\langle x(t)x(t+t_a)\rangle - \langle x(t)\rangle^2)/\sigma^2 = e^{-1}$. We take a delay $\tau = t_a = 174\ \Delta t$, which is smaller than the first zero of this function, $1250\ \Delta t$.

¶For large enough m, a plateau in Figs 7 (a) and (b), we have a slope ($q = 2$ in eq. (4))) $D_2 \approx \frac{\ln C_m(r)}{\ln (r)}$, where the correlation function is given in eq. (8) The average slope for $6 \leq m \leq 10$ is taken as D_2. Similarly, $K_2 \approx \frac{1}{3}\log_2\left[\frac{C_m(r)}{C_{m+3}(r)}\right]$ is the $q = 2$ entropy (base 2) in the same units as $\lambda_{\max}$ (bits per data sample), $8 \leq m \leq 10$.

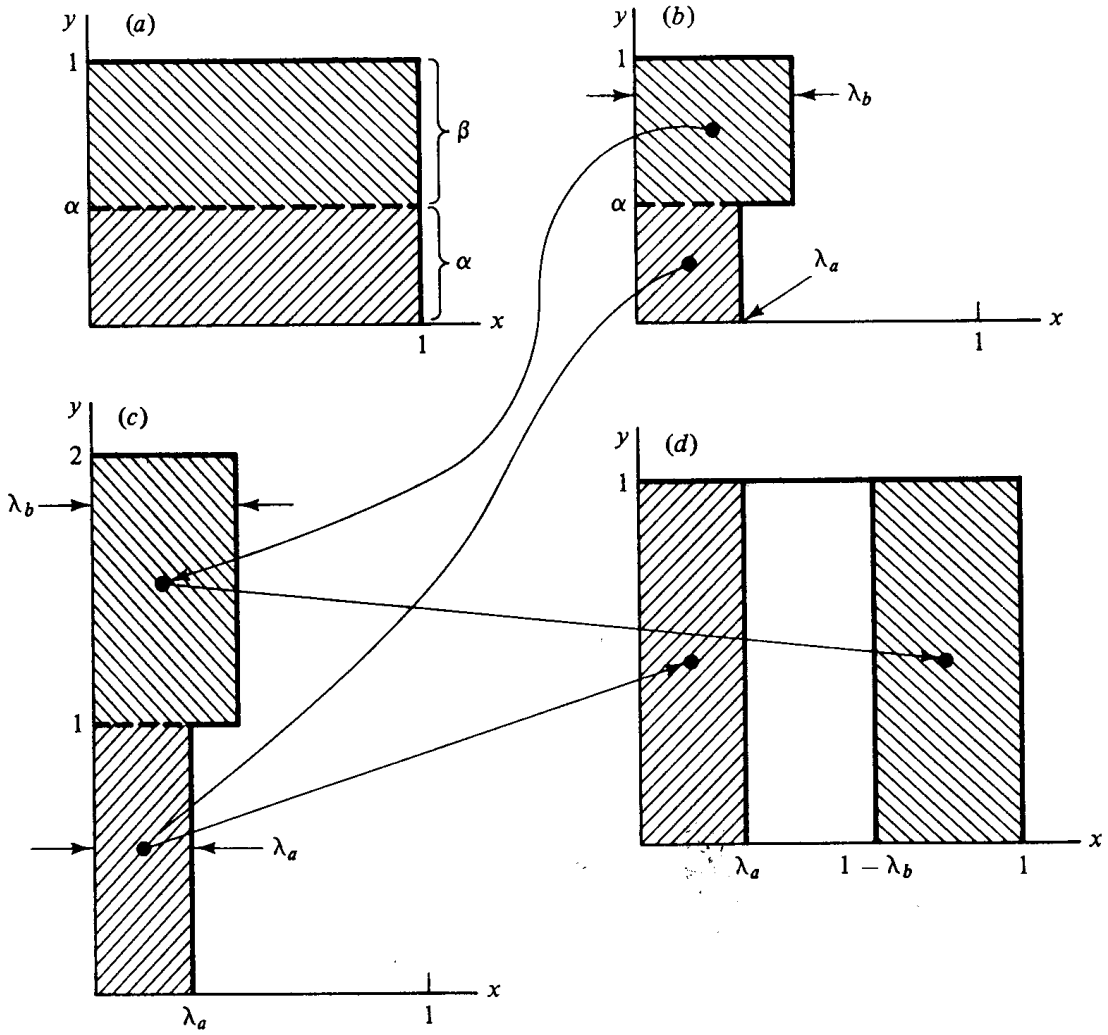

Fig. 6. Action of the generalized baker's map on the unit square.

The generalized self-similar baker's map (acting on the unit square) (Ott, 1993; Ott et al., 1994):

$$x_{n+1} = \begin{cases} sx_n & \text{for } y_n < p \\ (1-s) + sx_n & \text{for } y_n \geq p \end{cases}$$
$$y_{n+1} = \begin{cases} \frac{y_n}{p} & \text{for } y_n < p \\ \frac{y_n - p}{1-p} & \text{for } y_n \geq p \end{cases} \qquad (10)$$

Parameters:

- $p \leq 1/2$, natural invariant measure on the attractor of the system, the probability of visiting one region of the square (the probability of visiting the remaining region is $1 - p$).

- $s \leq 1/2$, folding and dissipation parameter (uniform compression, stretching and folding in the phase space).

For any q in Eq. (4) one has for the generalized dimension of the attractor (projected onto one axis)

$$(q-1)D_q = \frac{\log[p^q + (1-p)^q]}{\log s}. \tag{11}$$

No dissipation ($s = 1/2$):
the multifractal cascade $p-$model for fully developed turbulence,
the generalized weighted Cantor set (Meneveau and Sreenivasan, 1987).

The usual middle one-third Cantor set (without any multifractality):
$p = 1/2$ and $s = 1/3$.

The difference of the maximum and minimum dimension
(the least dense and most dense points on the attractor)

$$D_{-\infty} - D_{+\infty} = \frac{\log(1/p - 1)}{\log\,(1/s)} \tag{12}$$

In the limit $p \to 0$ this difference rises to infinity (degree of multifractality).

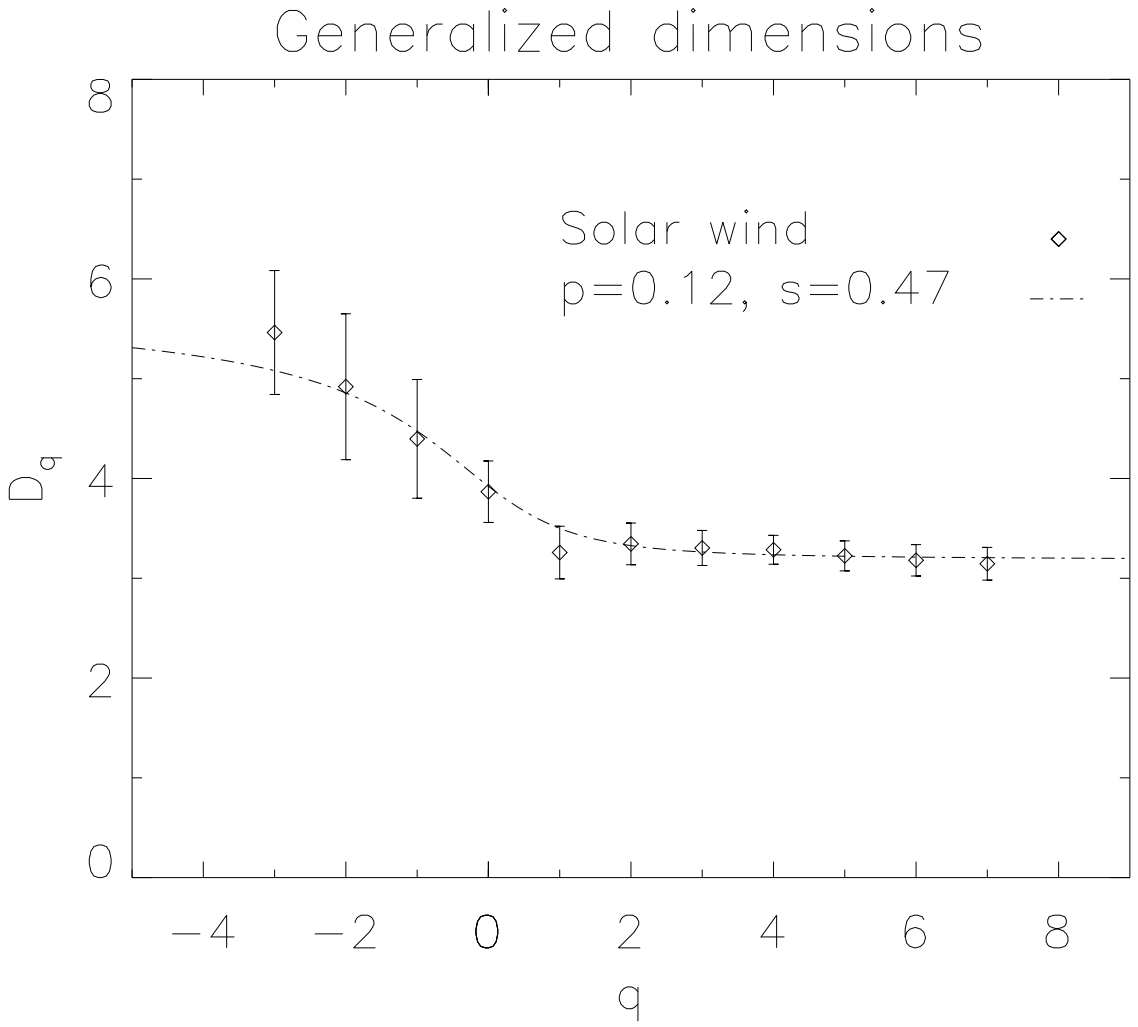

Fig. 7. The generalized dimensions D_q in Eq. (4) as a function of q. The correlation dimension is $D_2 = 3.4 \pm 0.2$, see Table 1. The values of $D_q + 3$ calculated analytically for the weighted baker's map with $p = 0.12$ and $s = 0.47$ (dash-dotted).

Conclusions

- The system is likely to have an *attractor* lying in the inertial manifold of low-dimension (probably between three and four).
- We have shown that the singular-value decomposition filter removes some amount of noise, which is sufficient to calculate the generalized dimensions of the solar wind attractor reconstructed in the phase space.
- The obtained multifractal spectrum of this attractor is consistent with that for the multifractal measure on the self-similar weighted baker's map. The action of this map exhibits stretching and folding properties leading to sensitive dependence on initial conditions.
- The values of the parameters fitted demonstrates small dissipation of the complex solar wind dynamical system and shows that some cubes that cover the attractor in phase space are visited at least one order of magnitudes more frequently than other cubes.
- The obtained characteristics of the attractor are significantly different from those of the surrogate data. Thus these results show multifractal structure of the solar wind in the inner heliosphere.

Hence we suggest that there exists an inertial manifold for the slow solar wind in the inner heliosphere in which the system has *multifractal* structure, and where noise is certainly not dominant.

This means that the observed irregular behaviour of the velocity and Alfvénic fluctuations results from intrinsic *nonlinear* dynamics rather than from random external forces.

The multifractal structure, convected by the wind, might probably be related to the complex topology shown by the magnetic field at the source regions of the solar wind.

References

[1] Hentschel, H. G. E., and Procaccia, I., Physica D, **8**, 435–444 (1983); Grassberger, P., Phys. Lett. A, **97**, 227–230 (1983); Halsey, T. C., Jensen, M. H., Kadanoff, L. P., Procaccia, I., and Shraiman, B. I., Phys. Rev. A, **33**, 1141–1151 (1986).

[2] Ott, E., *Chaos in Dynamical Systems*, Cambridge University Press, Cambridge, 1993.

[3] Ott, E., Sauer, T., and Yorke, J. A., *Coping with Chaos* (Wiley, New York, 1994).

[4] Mandelbrot, B. B., Multifractal measures, especially for the geophysicist, in *Pure and Applied Geophysics*, **131**, 5–42, Birkhäuser Verlag, Basel (1989).

[5] Burlaga, L. F., Geophys. Res. Lett., **18**, 69–72 (1991).

[6] Marsch, E., Tu, C. Y., Rosenbauer, H., Ann. Geophysicae, **14**, 259–269 (1996).

[7] Bruno, R., Carbone, V., Veltri, P., Pietropaolo, E., and Bavassano, B., Planet. Space Sci., **49**, 1201–1210 (2001).

[8] Schwenn, R., Large-scale structure of the interplanetary medium, in *Physics of the Inner Heliosphere*, edited by R. Schwenn and E. Marsch, Springer-Verlag, Berlin, 1990, Vol. 20, pp. 99–182.

[9] Macek, W. M., Physica D, **122**, 254–264 (1998).

[10] Macek W. M., and Redaelli, S., Phys. Rev. E, **62**, 6496–6501 (2000).

[11] Macek, W. M., Multifractality and chaos in the solar wind, in *Experimental Chaos*, edited by S. Boccaletti, B. J. Gluckman, J. Kurths, L. M. Pecora, and M. L. Spano, American Institute of Physics, New York, 2002, Vol. 622, pp. 74–79.

[12] A. M. Albano, J. Muench, C. Schwartz, A. I. Mess, and P. E. Rapp, Phys. Rev. A **38**, 3017–3026 (1988).

[13] Theiler, J., Eubank, S., Longtin, A., Galdrikian, B., and Farmer, J. D., Physica D, **58**, 77–94 (1992).

[14] Grassberger P., and Procaccia, I., Physica D, **9**, 189–208 (1983).

[15] Kaspar, F., and Schuster, H. G., Phys. Rev. A, **36**, 842–848 (1987).

[16] Theiler, J., Phys. Rev. A, **34**, 2427–2432 (1986).

[17] Meneveau, C., and Sreenivasan, K. R., Phys. Rev. Lett., **59**, 1424–1427 (1987).

[18] Kantz, H., Phys. Lett. A, **185**, 77–87 (1994).